ID: 14-0025; December 2014
DOI: 10.1530/ERP-14-0025

RESEARCH

The agreement between 3D, standard 2D and triplane 2D speckle tracking: effects of image quality and 3D volume rate

Tudor Trache, Stephan Stöbe, Adrienn Tarr, Dietrich Pfeiffer and **Andreas Hagendorff**

Department for Cardiology and Angiology, Leipzig University Hospital, Liebigstrasse 20, 04103 Leipzig, Germany

Correspondence should be addressed to T Trache
Email
tudor.trache@gmail.com

Abstract

Comparison of 3D and 2D speckle tracking performed on standard 2D and triplane 2D datasets of normal and pathological left ventricular (LV) wall-motion patterns with a focus on the effect that 3D volume rate (3DVR), image quality and tracking artifacts have on the agreement between 2D and 3D speckle tracking. 37 patients with normal LV function and 18 patients with ischaemic wall-motion abnormalities underwent 2D and 3D echocardiography, followed by offline speckle tracking measurements. The values of 3D global, regional and segmental strain were compared with the standard 2D and triplane 2D strain values. Correlation analysis with the LV ejection fraction (LVEF) was also performed. The 3D and 2D global strain values correlated good in both normally and abnormally contracting hearts, though systematic differences between the two methods were observed. Of the 3D strain parameters, the area strain showed the best correlation with the LVEF. The numerical agreement of 3D and 2D analyses varied significantly with the volume rate and image quality of the 3D datasets. The highest correlation between 2D and 3D peak systolic strain values was found between 3D area and standard 2D longitudinal strain. Regional wall-motion abnormalities were similarly detected by 2D and 3D speckle tracking. 2DST of triplane datasets showed similar results to those of conventional 2D datasets. 2D and 3D speckle tracking similarly detect normal and pathological wall-motion patterns. Limited image quality has a significant impact on the agreement between 3D and 2D numerical strain values.

Key Words
- 3D speckle tracking
- 2D speckle tracking
- image quality
- volume rate
- intermethod agreement

Introduction

The 2D speckle tracking (2DST) has been validated as a user-friendly and relatively robust method for the quantification of regional left-ventricular (LV) wall motion (1, 2, 3, 4, 5, 6, 7). 2DST strain measurements can also be performed on 2D triplane datasets in the same manner as in the standard, consecutively acquired 2D cineloops. In triplane datasets, all three standard apical views of the left ventricle are acquired in the same cardiac cycle using a 3D probe. Triplane echocardiography has been proven to be a reliable tool in the assessment of LV function as conventional 2D echocardiography, with the advantages of a faster data acquisition and a better standardisation of the apical views (7, 8, 9, 10). However, in 2D analyses, motion in and out of the visualised plane cannot be quantified, and appears as noise interfering with tracking (11, 12). Owing to its capacity to analyse the main vectors of the LV motion pattern as represented by the longitudinal, circumferential and radial strain within the

Table 1 Baseline characteristics of the study population. Considered cardiovascular risk factors were arterial hypertension, smoking, high blood cholesterol levels, diabetes and overweight.

	Minimum	Maximum	Mean	S.D.
Age	35	91	60	12.8
BMI	19.6	35.1	25.8	3.2
EF (%)	43	82	61.7	10.2
Heart rate at rest	46	107	70	12
Systolic blood pressure upon data acquisition	113	165	133.6	12.8
Diastolic blood pressure upon data acquisition	62	92	77.7	7.1
Number of cardiovascular risk factors				
Non-MI group	0	3	1.2	0.9
MI group	2	3	2.5	0.4

EF, ejection fraction; non-MI group, non-myocardial infarction group; MI group, myocardial infarction group.

same dataset, the 3DST emerges as a promising diagnostic method for the assessment of global and regional LV wall motion (13, 14, 15, 16, 17, 18), and previous research claimed its superiority over 2DST in quantification of normal wall-motion patterns and localising wall-motion abnormalities (11). In the 3DST analysis, the area strain combines the longitudinal and circumferential strain vectors, thus quantifying the variation of the surface of the analysed segment throughout the cardiac cycle. Its results have been shown to be consistent with LV wall-motion parameters such as the ejection fraction (EF) and wall-motion score index and with visual assessment of LV wall motion by experienced echocardiographers (19). The feasibility of area strain for the detection of early systolic dysfunction in heart failure patients has been demonstrated (20). Area strain has also been evaluated as a promising method for quantifying global LV mechanical dyssynchrony, thus as a potential additional parameter upon predicting success of cardiac resynchronisation therapy (21).

This study aims to test the agreement between 2DST on standard 2D and triplane 2D datasets, and 3DST. It was hypothesised that the image quality of the 3D datasets would influence the tracking quality and the results of the 3DST analyses and thus their correlation with 2DST. Upon data analysis, an influence of the volume rate of the 3D datasets (3DVR) on the intermethod agreement was detected. Although 3DVR was not regarded as an influential factor when the study was planned, its effects were analysed retrospectively, by postprocessing.

Methods

Study population and data acquisition

The study was designed as a prospective analysis. The patients were enrolled in addition to the initial cohort after beginning the data analysis. The total study population included 58 patients: three patients were excluded due to software failure to record all data required for the analysis. The remaining study population ($n=55$) was divided in two groups: the non-myocardial infarction (MI) group ($n=37$) included patients with no history of MI and with normal LV wall motion, undergoing echocardiography as a part of the clinical management of various conditions. The MI group ($n=18$) consisted of patients with previous anterior MI due to occlusion or narrowing of the left anterior descendent (LAD) artery, diagnosed by coronary angiography. All patients were in sinus rhythm at the time of data acquisition and had normal cardiac dimensions (left ventricular end diastolic volume (LVEDV) $=140\pm20$ ml). The baseline characteristics of the study population are given in Table 1. The comorbidities and relevant medications of the enrolled patients are given in Table 2. All patients underwent 2D and 3D transthoracic echocardiography at rest using a Vivid E9 scanner (GE Healthcare, Horten, Norway). The M5S probe was used to acquire the three standard apical long-axis 2D images of the left ventricle according to the actual recommendations (22). The mean temporal resolution of the 2D datasets was 59 ± 4 frames per second (fps). Triplane and 3D acquisitions were made from the apical position using the 4V probe. Triplane acquisitions are derived from the pyramidal data acquired with a 3D probe, from which the three standard apical cross-sections are extracted. The mean temporal resolution of the triplane acquisitions was 49 ± 5 fps. The 3D datasets were acquired during four or six cardiac cycles, depending on the spatial resolution and the cooperation of the patients. The pyramidal volume included

Table 2 Comorbidities and relevant medications of the enrolled patients.

	Non-MI group ($n=37$)	MI group ($n=18$)
Coronary heart disease	12 (32.4%)	18 (100%)
Diabetes	10 (27%)	8 (44.4%)
Hypertension	24 (64.8%)	15 (83.3%)
Rheumatic conditions (arthritis and Bechterew's disease)	3 (8.1%)	0
Renal insufficiency	5 (13.5%)	6 (33.3%)
Lupus	1 (2.7%)	0
High blood cholesterol	26 (70.2%)	18 (100%)
Use of β-blockers	14 (37.8%)	11 (61.1%)
Use of anti-hypertension drugs	24 (64.8%)	12 (66.6%)

the whole left ventricle. The 3D datasets had temporal resolutions ranging from 18 to 43 volumes/s (mean temporal resolution 29±5). The evaluation of the LVEF was made using the biplane planimetry according to the Simpson's method and the M-mode using the Teichholz method.

All patients gave consent to the study after full explanation of the purpose and nature of all procedures used. The investigation was approved by the Local Ethical Committee.

Speckle tracking analysis

All 2D and 3D speckle tracking analyses were performed offline using the EchoPAC Software version 112.0.0 (GE Healthcare). The analysed speckle tracking strain parameters included the global and segmental longitudinal strain detected on standard 2D, triplane 2D and 3D datasets, and the other strain vectors simultaneously quantified by 3DST analyses – circumferential, radial and area strain.

For the 2D strain analyses on standard 2D and triplane datasets, the Automated Function Imaging (AFI) programme (EchoPAC) was used. Topographic markers were manually set on each side of the mitral annulus and at the apex in all three apical standard views. The programme automatically tracked the endocardial border and calculated the myocardial region of interest (ROI) which was then tracked. Papillary muscles were included into the ventricular cavities and were not

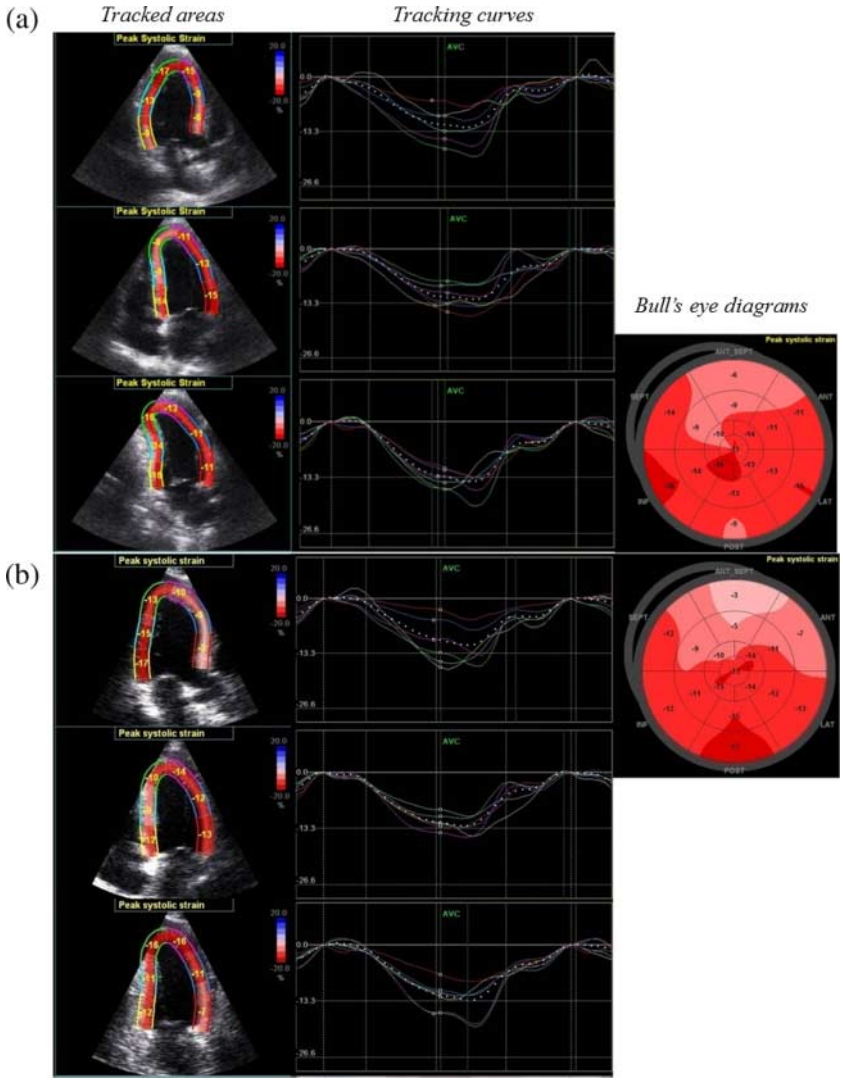

Figure 1
(a) Standard 2D longitudinal strain. (b) 2D triplane longitudinal strain. Examples of 2D speckle tracking (2DST) on standard (above) and triplane (below) datasets. The end of the systole (AVC, aortic valve closure) is marked.

part of the ROI. Where necessary, manual adjustments were made to the tracked endocardial border and/or to the ROI. The time markers required to identify end-diastolic and end-systolic frames were set with the help of pulsed-wave Doppler spectra of the LV outflow tract. The left ventricle was automatically divided into 17 segments according to the standard segmentation (23) and the segmental peak systolic strain (PeakSS) values were presented on colour-coded bull's eye diagrams (Fig. 1a and b).

The 3DST analyses were performed using the 4D left ventricular quantification (4DLVQ) function (EchoPAC). The software performed a semi-automated speckle tracking measurement of the LV myocardium. The endocardial border was detected on the end-systolic and end-diastolic frames of the dataset. In each of these frames, topographic markers were manually placed in the middle of the mitral valve and in the LV apex. The endocardial border was automatically delineated. Where necessary, manual adjustments were made. The software automatically calculated

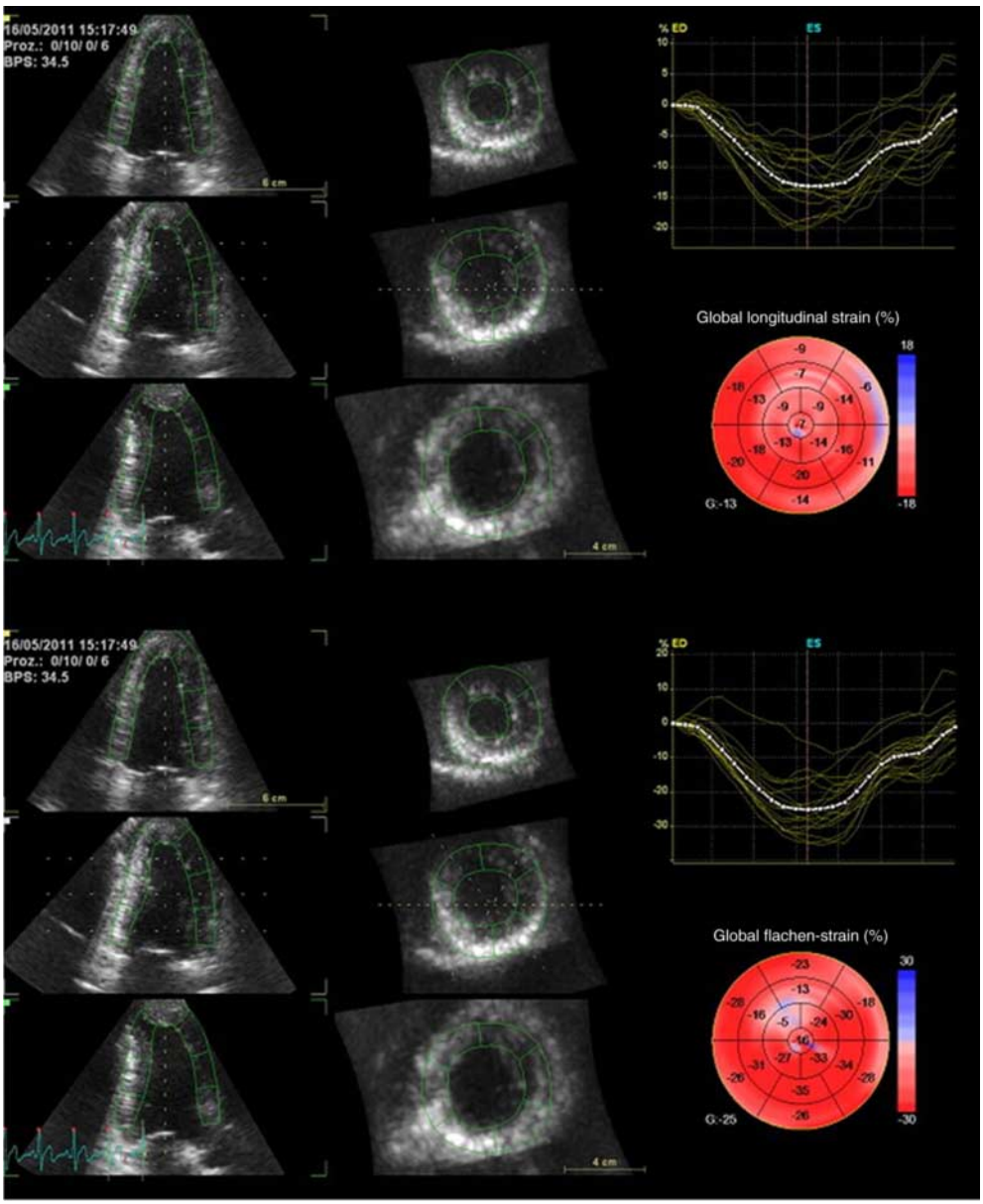

Figure 2
Examples of 3D speckle tracking analysis (longitudinal strain).

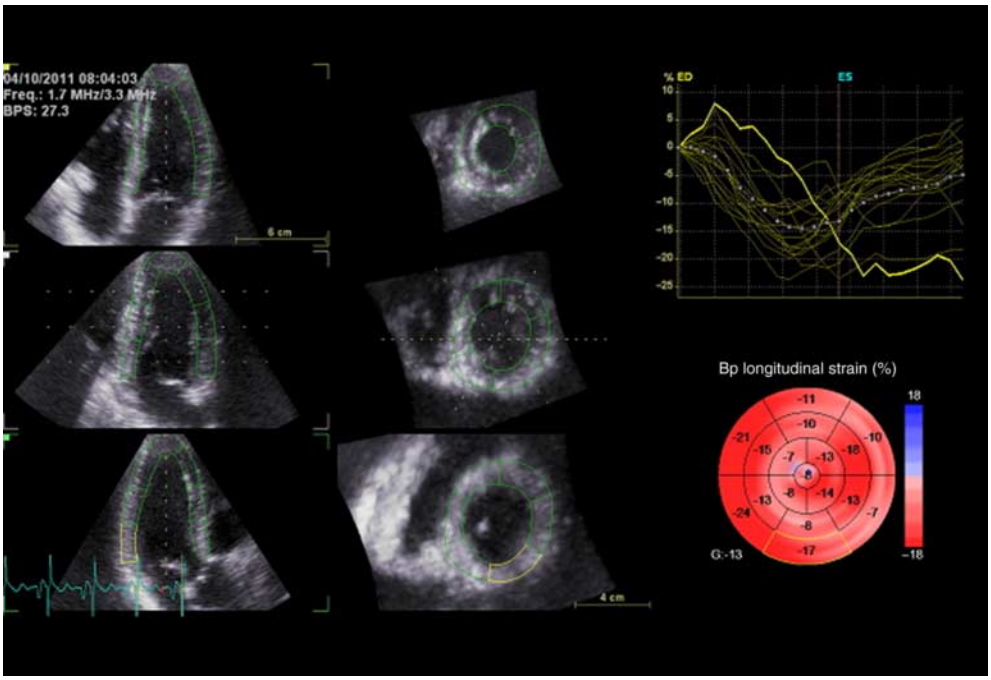

Figure 3
Examples of an abberrant 3D tracking curve due to image artifacts.

the LV volumes and computed the ROI for the speckle tracking. The endocardial and epicardial borders of the ROI were manually adjusted in order to ensure the inclusion of all myocardial segments in the strain analysis. All resulting strain curves were included into the analysis (Fig. 2). Cineloops containing the tracked areas, the bull's eye diagrams and the respective tracking curves, as well as the correspondent frozen end-systolic frames, were saved, and the tracking data were exported in the form of numerical matrices for further analysis. The 2D and 3D global strain values were automatically calculated by the used software, so that they were directly extracted and compared.

The segmental PeakSS values were computed differently by the 2DST and the 3DST algorithms. The AFI algorithm used for the 2DST analyses automatically calculated the PeakSS values for each segment and represented them together with the correspondent strain curves, whereas the 4DLVQ algorithm used for the 3DST analyses calculated the strain values for each frame of the analysed dataset. Therefore, the segmental PeakSS values of the 3D analyses were extracted from the numerical matrices of the 3D strain curves. The lowest strain value before the end-systolic frame was considered as the PeakSS value for the analysed segment and was stored for further analysis.

Interobserver variability

In order to test the interobserver variability, a total of ten patients with good image quality of the 3D datasets (six from the non-MI group and four from the MI group) were analysed in the same manner by a second operator, who was blinded to the results of the first measurement and to the diagnoses of the analysed patients.

Correlation analysis and statistical tests

Numerical analysis of strain values The strain values were tested for normal distribution using the Kolmogorov–Smirnov test. Linear regression and the Pearson's correlation coefficient were used to test the correlation between resting state global strain values and the LVEF in all enrolled patients. The agreement of global longitudinal strain (GLS) values detected by standard/triplane 2D and 3D speckle tracking was tested using linear regression and the method suggested by Bland & Altman (24). The significance of differences between standard 2D, triplane 2D and 3D GLS was tested using the paired samples *t*-test and the agreement between these parameters was tested using linear regression and the Pearson's correlation coefficient. Also, global strain values

Table 3 Correlation coefficients of the analysed strain parameters.

	Pearson's correlation coefficient	95% CI	*P* value
Standard 2D GLS – LVEF	−0.75	−0.84 to −0.60	<0.0001
Triplane 2D GLS – LVEF	−0.76	−0.85 to −0.61	<0.0001
GLS 3D – LVEF	−0.57	−0.73 to −0.36	<0.0001
GCS – LVEF	−0.57	−0.72 to −0.36	<0.0001
GAS – LVEF	−0.60	−0.75 to −0.40	<0.0001
GRS – LVEF	0.59	0.38 to 0.73	<0.0001

GLS, global longitudinal strain; GCS, global circumferential strain; GRS, global radial strain; GAS, global area strain; LVEF, left ventricular ejection fraction.

of patients from the non-MI group were compared with those of the MI group using the unpaired *t*-test.

In order to test the numerical agreement of segmental strain values in 2D and 3D speckle tracking measurements, the Pearson's correlation coefficient was used. The first analysis was performed using all detected strain values, and the correlations were recorded. For the second analysis, the image and tracking quality of the 3D and 2D triplane datasets were verified. Poor image quality was defined as i) endocardial border not traceable throughout the whole analysed systole and ii) segmental myocardium not visible throughout the whole analysed systole. It was observed that segments which were not visible throughout the whole cardiac cycle could not be properly analysed by the software and displayed aberrant tracking curves even though the peak strain values were within the expected range (Fig. 3). These segments displayed no relation between curve progression and phases of the cardiac cycle and were defined as segments with poor tracking quality. The strain values of segments with poor image and tracking quality were excluded from the numerical matrices, and correlation analysis was performed for the remaining segments.

3DVR – dependence of differences between 2D and 3D GLS Upon data analysis, it was observed that the agreement between 2D and 3D speckle tracking is dependent of the 3DVR datasets. This effect was assessed retrospectively by dividing the whole study population into two groups (3DVR <30, $n=25$ and 3DVR ≥ 30, $n=30$). The different volume rates can be mainly explained by the different cycle number during the acquisition modalities which were not prospectively planned in the acquisition protocol. Correlation analysis was performed for 2D and 3D GLS values in each group, and the paired samples *t*-test was used to test the statistical significance of differences between 2D and 3D GLS.

Comparative analysis of regional strain values in the MI-group

The segmental strain results of the patients in the MI group were grouped according to the three main coronary territories (25). The average strain values in each territory were compared with the other territories using the paired samples *t*-test.

Interobserver variability

The intraclass correlation coefficient (ICC), percentage and mean difference and s.d. between two separate measurements were used to test the interobserver variability of the speckle tracking. Percentage was defined as the absolute difference divided by the average of two measurements. The 2D and 3D speckle tracking measurements were performed as previously described by a second observer who was blinded to the results of the first measurement.

The statistical analyses and data plotting were performed using the MedCalc Software version 12 (MedCalc Software bvba, Ostend, Belgium). The Microsoft Excel (Microsoft Corporation) and the HDF Viewer (HDF Group, Champaign, IL, USA) software were used for the data export and organisation.

Results

Correlation analysis between 2D/3D global strain parameters and the LVEF

The Pearson's correlation coefficients between the 2D and 3D global strain values and the LVEF are given in Table 3. While the 2D GLS measured on monoplane and 2D triplane datasets showed good correlations with the LVEF, the 3D strain parameters correlated less. Even though only small differences were observed between the different 3D strain parameters, the global area strain (GAS) correlated best with the LVEF.

GLS values in non-MI and MI patients

The 2D and 3D GLS values in the MI group were consistently lower than those in the non-MI group, and the statistical significance of the differences between the two groups was confirmed by the *t*-test.

Correlation and comparative analysis of 2D/3D GLS

The linear regression diagrams of the standard/triplane 2D GLS and the 3D GLS are depicted in Fig. 4. Fig. 5 represents the corresponding Bland–Altman analysis, and

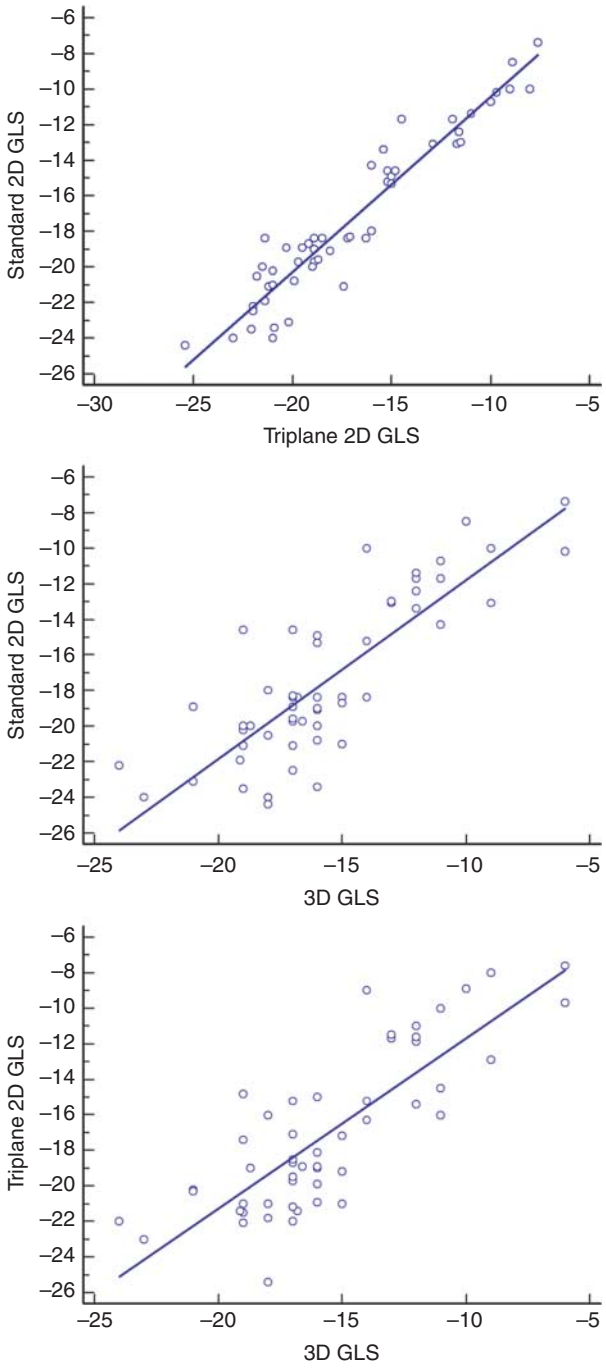

Figure 4
Regression diagrams of standard and triplane 2D global longitudinal strain (GLS) and 3D GLS.

the intermethod correlation coefficients can be found in Table 4.

Even though the correlations between the GLS values as measured with the three methods were very good, the Bland–Altman analysis revealed that the 2D GLS values measured on standard, as well as on triplane 2D datasets, were consistently higher than those of 3D GLS. The dispersion limits of the standard 2D vs triplane GLS analysis were significantly smaller than those of the standard/triplane 2D GLS vs 3D. Although the paired

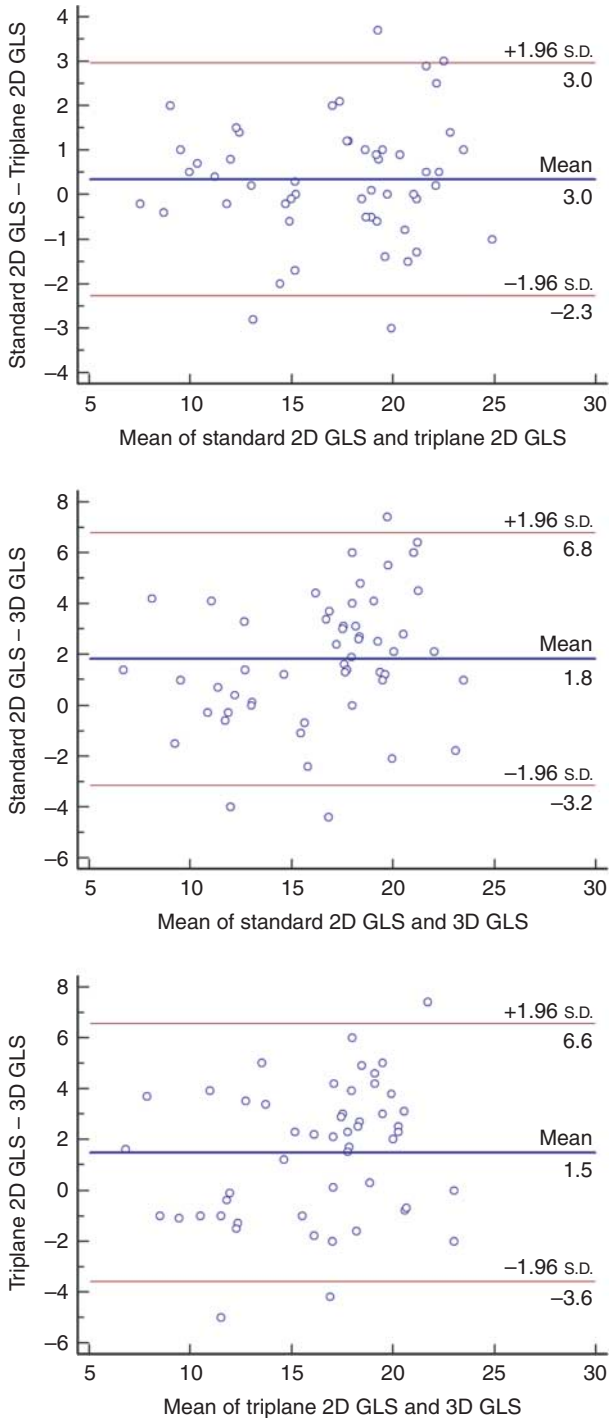

Figure 5
Bland–Altman plots of 2D global longitudinal strain (GLS) on standard and triplane 2D datasets and 3D-GLS.

Table 4 Correlation coefficients of standard, triplane 2D and 3D GLS.

	Pearson's correlation coefficient	95% CI	*P* value
2D standard GLS – 2D triplane GLS	0.95	0.92–0.97	<0.0001
2D standard GLS – 3D GLS	0.83	0.72–0.89	<0.0001
2D triplane GLS – 3D GLS	0.81	0.69–0.88	<0.0001

GLS, global longitudinal strain.

samples *t*-test revealed no significant differences between the values of standard and triplane 2D GLS, it sustained the observations of the Bland–Altman analysis and reveals the statistical significance of the differences between standard/triplane 2D GLS and the 3D GLS values.

3DVR – dependence of differences between 2D and 3D GLS

While there was no significant difference in correlation between standard and triplane 2D GLS values in the two groups selected by 3DVR, the correlation coefficients between standard/triplane 2D GLS and 3D GLS significantly differed in the two groups. Lower correlation coefficients were observed in the group with higher volume rates. The correlation coefficients between GLS values in the two groups are represented in Table 5, and the results of the unpaired *t*-test between standard 2D GLS and 3D GLS in the two groups are represented in Table 6. The Bland–Altman analysis of 2D and 3D GLS is shown in Fig. 6. The differences between 2D and 3D GLS were higher in the group with 3DVR higher than 30 volumes/s with comparable dispersion limits. In both groups, the standard 2D GLS had significantly higher absolute values than the 3D GLS.

Comparative analysis of segmental strain values

The correlation analysis of segmental PeakSS values performed using all detected data revealed rather moderate correlation coefficients, with a wide intertechnique variation of the exact segmental PeakSS values (Table 7). For a second analysis, the segments with poor 3D image quality and subsequent tracking artifacts were excluded according to the described criteria. From a total of 935 analysed segments, 112 (11.9%) were excluded. The regions from which most segments were excluded were the apical region ($n=52$, 46%), the basal anterior and lateral regions ($n=32$, 28%) and the basal anteroseptal region ($n=10$, 9%). The remaining 18 (16%) excluded segments were from the mid-anteroseptal and septal, mid-lateral and anterior, basal posterior and basal inferior regions. The exclusion of tracking artifacts due to poor image quality had a significant impact on intermethod correlations in all patients. Good correlations were found between the longitudinal PeakSS values of standard 2D and real-time triplane acquisitions, and the best correlation between 2D and 3D parameters was found between the 3D area strain and the standard 2D longitudinal strain.

Regional strain values in the MI-group

The analysis of regional strain values according to the main coronary territories in the MI group showed that all analysed 2D and 3D strain parameters detected lower regional strain values in the LAD territory compared with the other coronary territories. For all analysed strain parameters, the differences between the respective regional strain values were significant for the LAD vs left circumflex (LCX) and right coronary artery (RCA) territories. The differences between the LCX and the RCA territories were not statistically significant in the standard 2D and 3D longitudinal strain analyses and in the 3D area strain analysis. The 2D triplane longitudinal strain analysis revealed significantly higher regional strain values in the LCX territory. The results of the *t*-test analysis are represented in Table 8.

Interobserver variability

Table 9 gives the ICCs, the mean percentage variability and the mean differences between the measurements performed by two operators. Low percentage variability was observed, with smaller differences in standard and triplane 2D GLS measurements than in 3D measurements. Together with the high ICCs, these findings support a good interobserver agreement of the 2D/3D speckle tracking.

Table 5 2D/3D GLS correlations in the two 3DVR groups.

	3DVR <30 ($n=25$)	3DVR ≥30 ($n=30$)
Standard 2D GLS – Triplane 2D GLS	0.97	0.92
Standard 2D GLS – 3D GLS	0.86	0.71
Triplane 2D GLS – 3D GLS	0.85	0.67

GLS, global longitudinal strain; 3DVR, 3D volume rate. All correlations were statistically significant ($P<0.001$).

Table 6 Unpaired *t*-test in the two 3DVR groups.

	3DVR <30	3DVR ≥30
Correlation coefficient 2D GLS – 3D GLS	0.83	0.71
Mean difference	1.62	2.06
Standard deviation	2.60	2.49
95% CI	0.65–2.59	1.03–3.09
Two-tailed probability	$P=0.0019$	$P=0.0004$

3DVR, three-dimensional volume rate; GLS, global longitudinal strain.

Discussion

The feasibility of 2DST as a quantificator of global and regional LV function in different clinical situations has been repeatedly claimed (1). The used software has the potential of delivering fast results with exact numerical quantification of the movement of the analysed myocardial sections. Testing the feasibility of 3DST is a matter of interest, because this method has the capacity to follow movement not in a single plane of the tridimensional LV wall motion, but simultaneously in its whole volume. Thus, it overcomes the major limitation of the 2DST – the 'missing' of out-of-plane movement. Therefore, 3DST has the potential of delivering more accurate, complete real-time analyses of the complex tridimensional LV wall motion. Nevertheless, it is this more complex nature of the 3DST that makes its results more vulnerable to low image quality and tracking artifacts, and potentially prone to interactions with other parameters, such as the frame rate of the analysed 3D dataset (26, 27).

Triplane 2D datasets have the advantage of a simultaneous acquisition of all three standard apical views, so speckle tracking measurements on these datasets also have a clinical potential. Interchangeability of standard and triplane 2D acquisitions could not be demonstrated in previous research (27) due to differences between frame rates of standard and triplane acquisitions, and limited ability to obtain appropriate apical probe positions for good image acquisition. Upon acquisition of triplane data for this study, a main focus point was the standardisation of the apical views, in order to obtain accurate images of the left ventricle.

Under these prerequisites, 2DST measurements on triplane datasets correlated good with standard 2DST in our analysis. This may support the interchangeability of 2D conventional and triplane datasets if the triplane acquisitions are properly standardised.

The comparative analysis of 2D and 3D GLS values showed very good correlation coefficients between

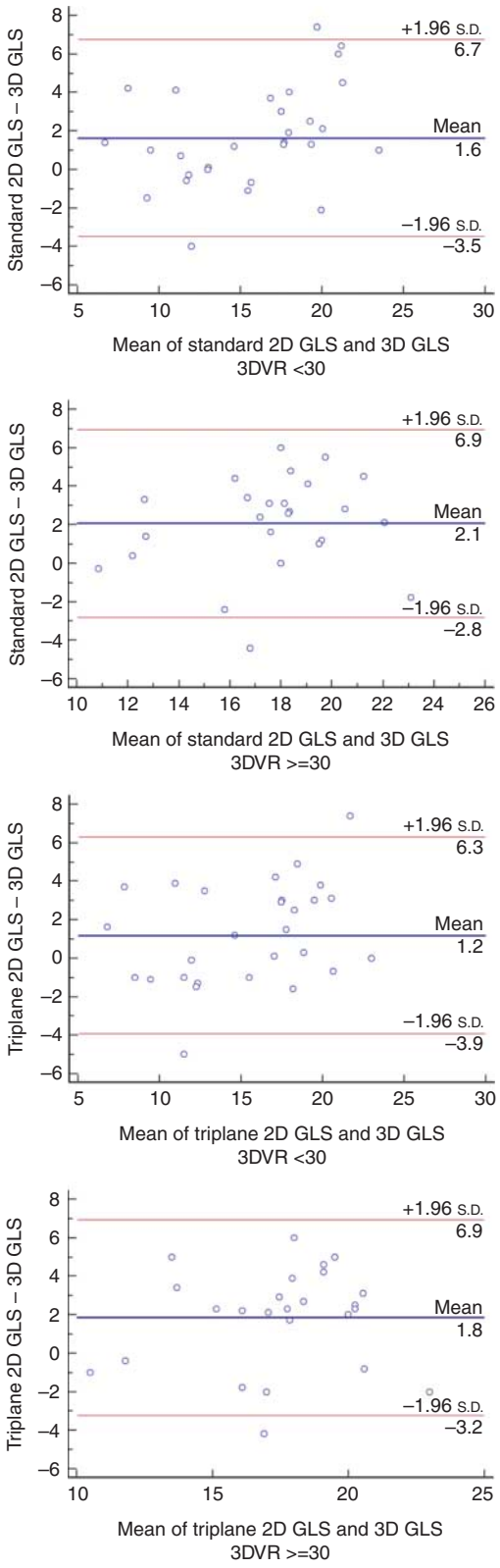

Figure 6
Bland–Altman plots of conventional and triplane 2D-GLS and 3D-GLS for 3DVR <30 and 3DVR ≥30 respectively.

Table 7 Mean correlation coefficients of PeakSS values before and after exclusion of tracking artifacts due to limited image quality (mean ± S.D.).

	Artifacts excluded	All segments
Area (3D) vs longitudinal (3D)	0.80 ± 0.11	0.73 ± 0.19
Area (3D) vs standard 2D	0.71 ± 0.07	0.38 ± 0.27
Area (3D) vs triplane 2D	0.66 ± 0.12	0.43 ± 0.24
Longitudinal (3D) vs standard 2D	0.58 ± 0.14	0.33 ± 0.28
Longitudinal (3D) vs triplane 2D	0.57 ± 0.14	0.32 ± 0.29
Standard 2D vs triplane 2D	–	0.66 ± 0.24

PeakSS, peak systolic strain.

standard/triplane 2D and 3D GLS. Nevertheless, a systematic bias was observed between the 2D and 3D measurements, which was also documented in other publications (15): the 3D GLS values were systematically lower than the 2D GLS values, with differences reaching statistical significance. This effect was explained as an effect of out-of-plane speckle patterns, as well as technical differences between the two methods.

Two possible implications were considered for the effects of 3DVR on the agreement between 2D and 3D speckle tracking: first, if the volume rate is too low, the resulting sampling bias would lead to an incomplete detection ('smoothing') of the strain curves in the 3D analysis, thus to loss of information and to lower and less accurate absolute strain values compared to the 2D analysis. This effect has been demonstrated by Yodwut *et al*. (26). Second, the image quality of 3D datasets becomes impaired at higher volume rates, because of lower line density, which may lead to higher differences between 2D and 3D strain measurements. The 3DVR at which significant information loss occurs has been stated somewhere between 10 and 18 volumes/s (26), and the volume rate at which a significant reduction in spatial resolution occurs has been described around 50 volumes/s (27). In this study, the differences between the 2D and the 3D measurements were higher in datasets with volume rates higher than 30 volumes/s. Also, the correlations between 2D and 3D GLS were slightly lower in datasets with volume rates higher than 30 volumes/s. This unexpected finding may be due to the 'trade-off' between temporal and spatial resolution. Although this effect was described as significant at higher volume rates, our analysis points to the fact that the 3DVR influences the agreement between 2D and 3D speckle tracking already at lower volume rates.

3D and 2D speckle tracking showed a similar capacity of detecting and localising impaired LV systolic function. All analysed strain parameters detected significantly lower global strain values in patients with previous anterior MI due to obstruction or narrowing of the LAD artery. In our MI group, we assumed that a cumulative effect on the regional wall motion would still be detectable in the LAD region, if the analysed methods similarly localised wall-motion abnormalities. The analysis of the numerical strain data confirmed this supposition and revealed significantly lower values in the LAD region than in the LCX/RCA regions. This supports the 3DST as an additional tool for the assessment of regional LV kinetics. Nevertheless, 3D and 2D speckle tracking are not interchangeable methods in the detection and quantification of regional wall-motion abnormalities.

One of the important points of this study upon validating 3DST against 2DST is the role of the image quality of the 3D datasets. Although 3D global strain parameters show very good correlations with their 2D counterparts, the effect of poor image quality on the reliability of 3D tracking results could be demonstrated by the differences in the more detailed correlation analysis of the segmental PeakSS values. The accuracy of 3DST-derived segmental strain values is significantly influenced by the image quality of the analysed dataset. This is also a finding that does not support the interchangeability of 2D and 3D speckle tracking. Segments with aberrant tracking curves due to low image quality were predominantly found in the apical region (probably due

Table 8 *t*-test between regional strain values according to the coronary territories in the MI group.

	2D standard longitudinal strain			2D triplane longitudinal strain			3D longitudinal strain			3D area strain		
	LAD	RCA	LCX	LAD	RCA	LCX	LAD	RCA	LCX	LAD	RCA	LCX
Mean regional strain value	0.115	0.176	0.198	0.116	0.163	0.201	0.118	0.176	0.205	0.21	0.31	0.35
Variance	0.0005	0.0004	0.0005	0.0007	0.0005	0.0004	0.0004	0.0005	0.0005	0.0007	0.002	0.0005
Two-tailed probability	<0.001	<0.001	0.051	<0.001	<0.001	0.002	<0.001	0.04	0.38	<0.001	<0.001	0.09

LAD, left anterior descending; LCX, left circumflex; RCA, right coronary artery.

Table 9 Interobserver variability of speckle-tracking measurements ($n=10$).

	ICC	Percentage variability	Mean difference ± s.d.
Standard 2D GLS	0.98	4.71 ± 3.37	−0.01 ± 0.92
Triplane 2D GLS	0.98	4.8 ± 3.04	−0.21 ± 0.90
3D GLS	0.94	8.09 ± 2.28	−0.46 ± 1.25
3D GCS	0.97	5.74 ± 5.55	0.72 ± 1.01
3D GAS	0.91	9.96 ± 23.34	1.16 ± 3.47
3D GRS	0.97	6.36 ± 14.45	1.66 ± 3.38

ICC, intraclass correlation coefficient.

to close-field image artifacts), in the basal anterior, lateral and to a lesser extent in the anteroseptal regions (probably as a result of the interposition of the left lung). The number of segments with poor image quality in the posterior and inferior basal regions and the mid regions was significantly lower, probably due to the favourable anatomic situation of these regions.

The analysed 2D datasets were highly standardised, and the 2D and 3D speckle tracking for the interobserver variability were performed by the second operator by the same quality criteria in respect to the optimal adjustment of the ROI to include the whole ventricular wall and correct placement of the end-systolic and end-diastolic markers. This may explain the low interobserver variability in this study, and points to a good reproductibility of 2D and 3D speckle tracking if these prerequisites are met.

Correlation analysis of 2D/3D global strain and the LVEF was performed despite the fact that these parameters contain different physiological information. LVEF represents the volumetric fraction of blood volume which is pumped out of the left ventricle during every heartbeat. This volumetric fraction depends on the size of the ventricle, the contraction of the myocardial fibers, integrity of the mitral and aortic valves as well as the diastolic function. On the other hand, the global strain reflects the fractional change in the respective LV dimension, comparing the maximum contracting state at systole with the end-diastolic dimension. Both parameters, however, are pre- and postload dependent.

In this study, correlation analysis between the EF and the global strain parameters was performed for normally contracting hearts with normal dimensions as well as hearts with MI with comparable cardiac dimensions. Furthermore, no relevant valvular heart disease and no severe diastolic dysfunction were present in these patients. Under these circumstances, both 2D and 3D global strain parameters showed good correlations with the LVEF. While the 2D monoplane and triplane longitudinal strain showed better correlations with the EF, the best correlation with 3D strain parameters was observed for the GAS.

Limitations

This study aims a detailed comparison of 2D and 3D speckle tracking with respect of the volume rate and image quality of the 3D datasets, with correlation analysis of segmental PeakSS values. Yet, the analysis of 2D and 3D tracking data is not performed in the same way. 2D PeakSS values were automatically calculated, whereas 3D PeakSS values had to be manually extracted from the 3D analyses. This could be a limitation, because the compared 2D–3D PeakSS values were not calculated by the same algorithm in a relatively small study cohort. It was attempted to test the capacity of the analysed methods to similarly localise the contraction deficit in a group of patients with angiographically diagnosed LAD-occlusion. Given the well-known variations of the coronary tree anatomy, the results yielded from the comparison of regional strain values from standardised coronary territories must be seen as approximations more than as exact correlation parameters. A comparison of regional strain values of segments grouped according to individual coronary tree anatomy could deliver a more accurate insights into this issue. The effect of aberrant 3D segmental tracking curves on the global strain curves in the 3D analysis was not accounted for. This is a potential source of error upon validating 3D global strain as an accurate parameter for the LV systolic function.

Conclusion

The image quality and 3DVR datasets seem to have a significant impact on the accuracy of the strain measurements. An important conclusion of this study is that common protocols of data acquisition regarding standardisation of views, frame or volume rate and image quality should be prerequisites in future studies of echocardiographic LV deformation imaging.

Also, due to the faster data acquisition and interchangeability with the standard 2DST measurements, 2DST on triplane datasets can be validated as a reliable method for the quantification of the LV systolic function, if a good image quality and standardisation of the analysed datasets are given. 3DST shows good agreement with the 2DST, rendering area strain as a reliable parameter. Nevertheless, the two methods are not interchangeable.

Declaration of interest
The authors declare that there is no conflict of interest that could be perceived as prejudicing the impartiality of the research reported.

Funding
This research did not receive any specific grant from any funding agency in the public, commercial or not-for-profit sector.

References

1 Mor-Avi V, Lang RM, Badano LP, Belohlavek M, Cardim NM, Derumeaux G, Galderisi M, Marwick T, Nagueh SF, Sengupta PP *et al*. 2011 Current and evolving echocardiographic techniques for the quantitative evaluation of cardiac mechanics: ASE/EAE Consensus Statement on Methodology and Indications Endorsed by the Japanese Society of Echocardiography. *European Journal of Echocardiography* **12** 167–205. (doi:10.1093/ejechocard/jer021)

2 Manovel A, Dawson D, Smith B & Nihoyannopoulos P 2010 Assessment of left ventricular function by different speckle-tracking software. *European Journal of Echocardiography* **11** 417–421. (doi:10.1093/ejechocard/jep226)

3 Amundsen BH, Helle-Valle T, Edvardsen T, Torp H, Crosby J, Lyseggen E, Stoylen A, Ihlen H, Lima JA, Smiseth OA *et al*. 2006 Noninvasive myocardial strain measurement by speckle tracking echocardiography: validation against sonomicrometry and tagged magnetic resonance imaging. *Journal of the American College of Cardiology* **47** 789–793. (doi:10.1016/j.jacc.2005.10.040)

4 Adamu U, Schmitz F, Becker M, Kelm M & Hoffmann R 2009 Advanced speckle tracking echocardiography allowing a three-myocardial layer-specific analysis of deformation parameters. *European Journal of Echocardiography* **10** 303–308. (doi:10.1093/ejechocard/jen238)

5 Lafitte S, Perlant M, Reant P, Serri K, Douard H, DeMaria A & Roudaut R 2009 Impact of impaired myocardial deformations on exercise tolerance and prognosis in patients with asymptomatic aortic stenosis. *European Journal of Echocardiography* **10** 414–419. (doi:10.1093/ejechocard/jen299)

6 Cimino S, Canali E, Petronilli V, Cicogna F, De Luca L, Francone M, Sardella G, Iacoboni C & Agati L 2013 Global and regional longitudinal strain assessed by two-dimensional speckle tracking echocardiography identifies early myocardial dysfunction and transmural extent of myocardial scar in patients with acute ST elevation myocardial infarction and relatively preserved LV function. *European Heart Journal Cardiovascular Imaging* **14** 805–811. (doi:10.1093/ehjci/jes295)

7 Fontana A, Zambon A, Cesana F, Giannattasio C & Trocino G 2012 Tissue Doppler, triplane echocardiography, and speckle tracking echocardiography: different ways of measuring longitudinal myocardial velocity and deformation parameters. A comparative clinical study. *Echocardiography* **29** 428–437. (doi:10.1111/j.1540-8175.2011.01618.x)

8 Nucifora G, Badano LP, Dall'Armellina E, Gianfagna P, Allocca G & Fioretti PM 2009 Fast data acquisition and analysis with real time triplane echocardiography for the assessment of left ventricular size and function: a validation study. *Echocardiography* **26** 66–75. (doi:10.1111/j.1540-8175.2008.00762.x)

9 Malm S, Frigstad S, Sagberg E, Steen PA & Skjarpe T 2006 Real-time simultaneous triplane contrast echocardiography gives rapid, accurate, and reproducible assessment of left ventricular volumes and ejection fraction: a comparison with magnetic resonance imaging. *Journal of the American Society of Echocardiography* **19** 1494–1501. (doi:10.1016/j.echo.2006.06.021)

10 Ren M, Tian JW, Leng XP, Wang HM, Wang Y & Wang ZZ 2009 Assessment of global and regional left ventricular function after surgical revascularization in patients with coronary artery disease by real-time triplane echocardiography. *Journal of Ultrasound in Medicine* **28** 1175–1184.

11 Maffessanti F, Nesser HJ, Weinert L, Steringer-Mascherbauer R, Niel J, Gorissen W, Sugeng L, Lang RM & Mor-Avi V 2009 Quantitative evaluation of regional left ventricular function using three-dimensional speckle tracking echocardiography in patients with and without heart disease. *American Journal of Cardiology* **104** 1755–1762. (doi:10.1016/j.amjcard.2009.07.060)

12 de Isla LP, Vivas D & Zamorano JL 2008 Three-dimensional speckle tracking. *Current Cardiovascular Imaging Reports* **1** 25–29. (doi:10.1007/s12410-008-0006-1)

13 Nesser JH, Mor-Avi V, Gorissen W, Weinert L, Steringer-Mascherbauer R, Niel J, Sugeng L & Lang RM 2009 Quantification of left ventricular volumes using three-dimensional echocardiographic speckle tracking: comparison with MRI. *European Heart Journal* **30** 1565–1573. (doi:10.1093/eurheartj/ehp187)

14 Kleijn SA, Aly MF, Terwee CB, van Rossum AC & Kam O 2011 Reliability of left ventricular volumes and function measurements using three-dimensional speckle tracking echocardiography. *European Journal of Echocardiography* **12** 159–168. (doi:10.1093/ejechocard/jer174)

15 Reant P, Barbot L, Touche C, Dijos M, Arsac F, Pillois X, Landelle M, Roudaut R & Lafitte S 2012 Evaluation of global left ventricular systolic function using three-dimensional echocardiography speckle-tracking strain parameters. *Journal of the American Society of Echocardiography* **25** 68–79. (doi:10.1016/j.echo.2011.10.009)

16 Lilli A, Baratto MT, Del Meglio J, Chioccioli M, Magnacca M, Svetlich C, Ottonelli AG, Poddighe R, Comella A & Casolo G 2011 Three-dimensional simultaneous strain-volume analysis describes left ventricular remodelling and its progression: a pilot study. *European Journal of Echocardiography* **12** 520–527. (doi:10.1093/ejechocard/jer073)

17 Kleijn SA, Brouwer WP, Ali MF, Rüssel IK, de Roest GJ, Beek AM, van Rossum AC & Kamp O 2012 Comparison between three-dimensional speckle-tracking echocardiography and cardiac magnetic resonance imaging for quantification of left ventricular volumes and function. *European Heart Journal Cardiovascular Imaging* **13** 834–839. (doi:10.1093/ehjci/jes030)

18 Duan F, Xie M, Wang X, Li Y, He L, Jiang L & Fu Q 2012 Preliminary clinical study of left ventricular myocardial strain in patients with non-ischemic dilated cardiomyopathy by three-dimensional speckle tracking imaging. *Cardiovascular Ultrasound* **10** 8. (doi:10.1186/1476-7120-10-8)

19 Kleijn SA, Aly MF, Terwee CB, van Rossum AC & Kamp O 2011 Three-dimensional speckle tracking echocardiography for automatic assessment of global and regional left ventricular function based on area strain. *Journal of the American Society of Echocardiography* **24** 314–321. (doi:10.1016/j.echo.2011.01.014)

20 Wen H, Liang Z, Zhao Y & Yang K 2011 Feasibility of detecting early left ventricular systolic dysfunction using global area strain: a novel index derived from threedimensional speckle-tracking echocardiography. *European Journal of Echocardiography* **12** 910–916. (doi:10.1093/ejechocard/jer162)

21 Thebault C, Donal E, Bernard A, Moreau O, Schnell F, Mabo P & Leclercq C 2011 Real-time three-dimensional speckle tracking echocardiography: a novel technique to quantify global left ventricular mechanical dyssynchrony. *European Journal of Echocardiography* **12** 26–32. (doi:10.1093/ejechocard/jeq095)

22 Lang RM, Bierig M, Devereux RB, Flachskampf FA, Foster E, Pellikka PA, Picard MH, Roman MJ, Seward J, Shanewise J *et al*. 2006 Recommendations for chamber quantification. *European Journal of Echocardiography* **7** 79–108. (doi:10.1016/j.euje.2005.12.014)

23 Cerqueira MD, Weissman NJ, Dilsizian V, Jacobs AK, Kaul S, Laskey WK, Pennell DJ, Rumberger JA, Ryan T, Verani MS *et al*. 2002 Standardized myocardial segmentation and nomenclature for tomographic imaging of the heart: a statement for healthcare professionals from the Cardiac Imaging Committee of the Council on Clinical Cardiology of the

American Heart Association. *Circulation* **105** 539–542. (doi:10.1161/hc0402.102975)

24 Bland JM & Altman DG 1986 Statistical methods for assessing agreement between two methods of clinical measurement. *Lancet* **1** 307–310. (doi:10.1016/S0140-6736(86)90837-8)

25 Loukas M, Sharma A, Blaak C, Sorenson E & Mian A 2013 The clinical anatomy of the coronary arteries. *Journal of Cardiovascular Translational Research* **6** 197–207. (doi:10.1007/s12265-013-9452-5)

26 Yodwut C, Weinert L, Klas B, Lang RM & Mor-Avi V 2012 Effects of frame rate on three-dimensional speckle-tracking-based measurements of myocardial deformation. *Journal of the American Society of Echocardiography* **25** 978–985. (doi:10.1016/j.echo.2012.06.001)

27 Negishi K, Negishi T, Agler DA, Plana JC & Marwick TH 2012 Role of temporal resolution in selection of the appropriate strain technique for evaluation of subclinical myocardial dysfunction. *Echocardiography* **29** 334–339. (doi:10.1111/j.1540-8175.2011.01586.x)

Received in final form 29 October 2014
Accepted 4 November 2014